Comparative study of 3-dimensional woven joint architectures for composite spacecraft structures

Justin S. Jones, Daniel L. Polis, Kenneth N. Segal
National Aeronautics and Space Administration
Goddard Space Flight Center
Greenbelt, MD 20771

ABSTRACT

The National Aeronautics and Space Administration (NASA) Exploration Systems Mission Directorate initiated an Advanced Composite Technology (ACT) Project through the Exploration Technology Development Program in order to support the polymer composite needs for future heavy lift launch architectures. As an example, the large composite structural applications on Ares V inspired the evaluation of advanced joining technologies, specifically 3D woven composite joints, which could be applied to traditionally manufactured barrel segments. Implementation of these 3D woven joint technologies may offer enhancements in damage tolerance without sacrificing weight. However, baseline mechanical performance data is needed to properly analyze the joint stresses and subsequently design/down-select a preform architecture. Six different configurations were designed and prepared for this study; each consisting of a different combination of warp/fill fiber volume ratio and preform interlocking method (z-fiber, fully interlocked, or hybrid). Tensile testing was performed for this study with the enhancement of a dual camera Digital Image Correlation (DIC) system which provides the capability to measure full-field strains and three dimensional displacements of objects under load. As expected, the ratio of warp/fill fiber has a direct influence on strength and modulus, with higher values measured in the direction of higher fiber volume bias. When comparing the z-fiber weave to a fully interlocked weave with comparable fiber bias, the z-fiber weave demonstrated the best performance in two different comparisons. We report the measured tensile strengths and moduli for test coupons from the 6 different weave configurations under study.

1. INTRODUCTION

1.1 Purpose

The NASA Advanced Composites Technologies (ACT) program seeks to provide alternative composite material solutions for flight vehicles that offer weight savings without sacrificing reliability or improving reliability without sacrificing weight. One step in this direction is the development of 3D woven H-preform joints for connecting large shell structures; providing a replacement for more traditional double lap joints. Figure 1 shows a traditional double lap joint, as recently implemented on the NASA Engineering and Safety Center's (NESC) Composite Crew Module, versus a 3D woven H-preform replacement, as shown in a joint coupon in Figure 2. In this application, 3D woven composites may improve the damage tolerance of these joints, essentially increasing reliability without sacrificing weight.

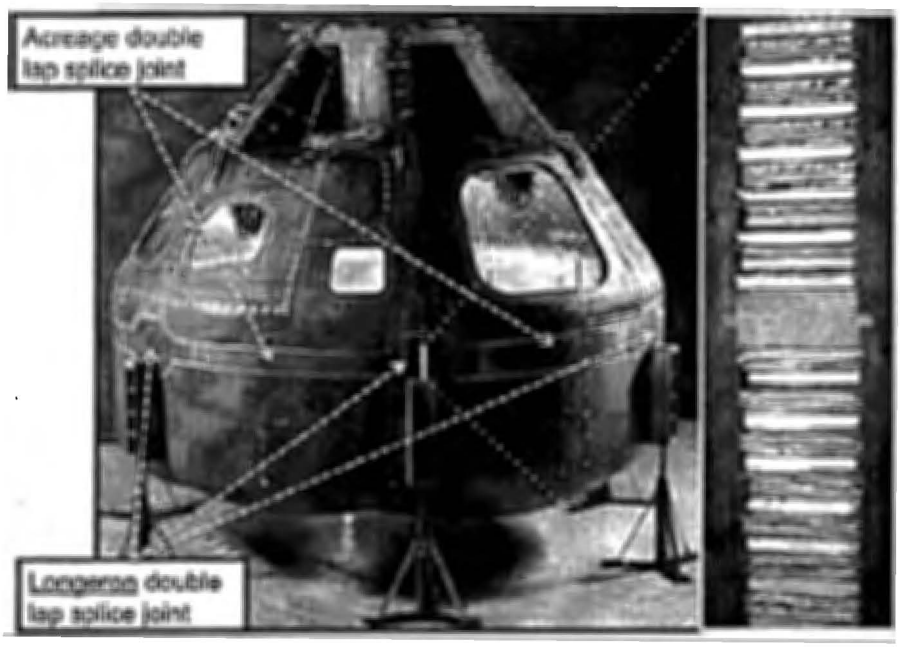

Figure 1: NASA Engineering and Safety Center's (NESC) Composite Crew Module, showing a traditional double lap splice joint of upper and lower sandwich shells.

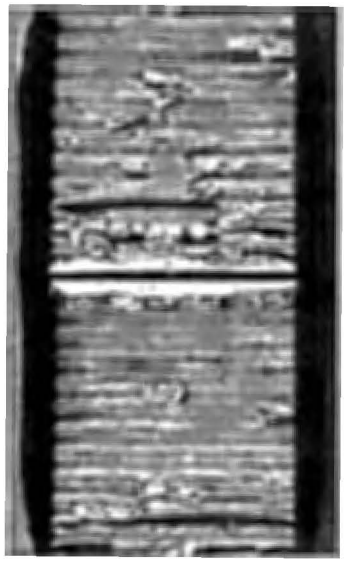

Figure 2: 3D woven H-preform joint coupon of two inch thick sandwich.

Prior to designing and implementing a full-scale H-preform joint, baseline mechanical performance data is needed to properly down-select the weave architecture. Toward this end, this study evaluates six different weave designs; each with a different combination of warp/fill fiber tow volume ratio and through-thickness interlocking. This paper reports the measured tensile strengths and moduli for test coupons from these weave configurations under study. Values are reported for both the fill fiber direction of the H-preform cap surface (direction across

the joint intersection) and the warp fiber direction of the cap surface (direction along the joint intersection).

1.2 Overview of Weave Configurations

The six 3D weave configurations of interest in this study involve varying warp to fill fiber ratios and one of three general fiber architectures. Each H-preform configuration consists of two faces, or caps, each with 6 layers of IM7 fiber (PAN-based, intermediate modulus carbon fiber produced by Hexcel, 12K filament count tows) that are coupled together with a thin web section that creates the H shape. The two main fiber architectures are the fully interlocked weave and the Z-fiber weave. A third architecture (found in Weave 2) is a hybrid of the two. The fully interlocked weave consists of a 3-dimensional 1-harness design in which each ply is bound to its neighbor through an orthogonal fiber which crosses over or under every tow. The Z-fiber design achieves ply cohesion through a z-tow which passes straight through the thickness of the cap layup. A summary of the weave configurations is shown in Table 1.

Table 1: Description of the six weave architectures used in this study.

Weave #	Warp/Fill Fiber Ratio	Architecture
1	50/50	Fully Interlocked
2	50/50	Hybrid
3	50/50	Z-fiber
4	25/75	Z-fiber
5	75/25	Z-fiber
6	25/75	Fully Interlocked

Prior to the testing reported in this article, all of the H-preforms were fully infused and cured with MTM®45-1 resin, which is a toughened epoxy produced by Advanced Composites Group. Figure 3 contains an image of weave 1 prior to resin infusion. All the performs were woven by Bally Ribbon Mills (Bally, PA).

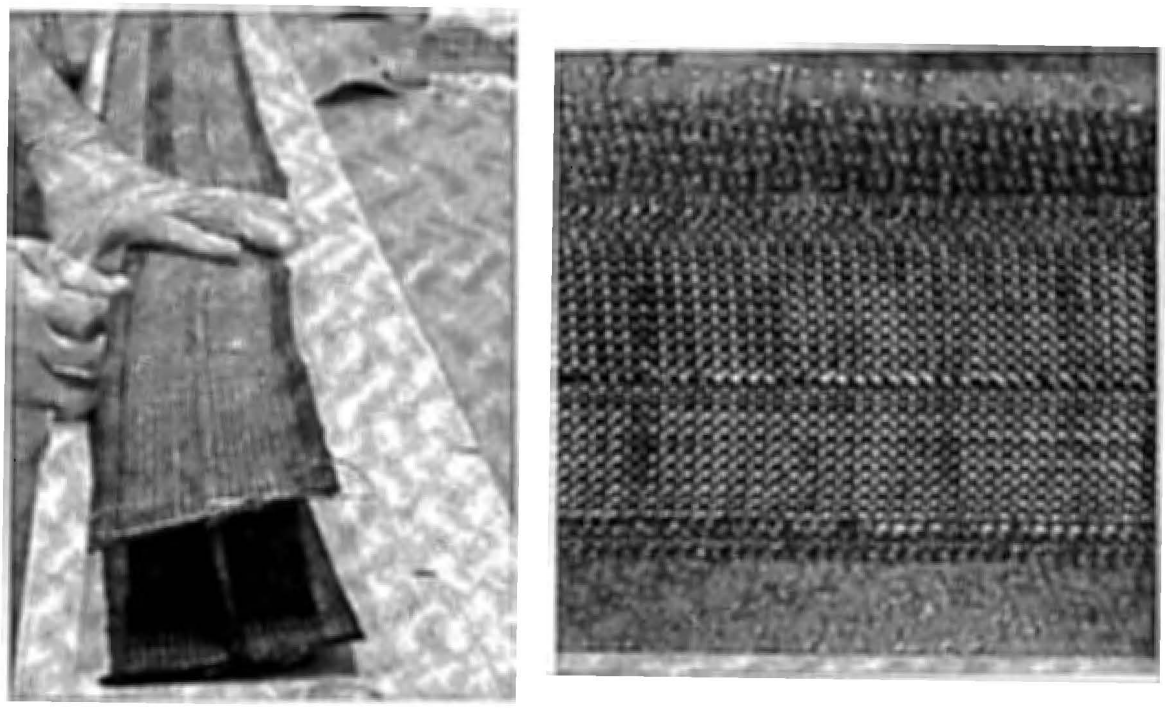

Figure 3: Example of an H-preform prior to resin infiltration. The image on the left shows the full preform and the right image shows the cap of a fully interlocked preform.

2. EXPERIMENTATION

2.1 Sample Preparation

In order to obtain H-preform specimens for characterization, each unique weave was infused and cured in a single step. Rather than infusing and curing with sandwich panels inserted into the H-preform, as shown in Figure 2, release coated tooling was used. This enabled the joining process to be simulated but produced a free-standing cured H-preform coupon. These infusion coupons were produced in lengths of approximately eight inches in length. These coupons were sectioned into 1" wide samples using a Struers® Exotom-M chop saw. For each of the H-preforms, samples were sectioned so that at least 4 coupons were extracted from the cap in the warp fiber direction and at least four samples were extracted from the cap—across the joint—in the fill fiber direction. Figure 4 shows a 1" wide cross-section of a free-standing H-preform that provided two fill direction coupons, which were released from one another by cutting the thin web section that connects them. For illustration, the warp fiber direction is also noted in the image. For the warp direction samples, the sections were chosen such that they excluded the tapered edges and areas within ¼" from the web.

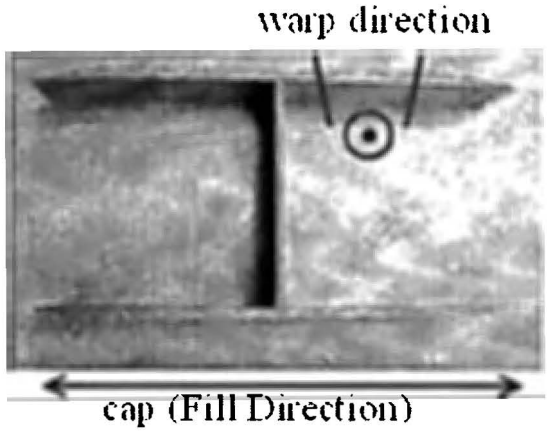

Figure 4: Cross-section of H-preform showing the fill and warp fiber directions that were isolated during mechanical tests.

Once the samples were sectioned, grip tabs were applied by bonding 1" x 1" x 1/16" thick G10 composite to both sides of each end of the samples using Hysol® EA 9309.2 epoxy. The epoxy was cured at 80°C for 1 hour. The sides of the samples were then lightly sanded to remove any excess epoxy or irregularities. Lastly, the front surface was painted with a black and white stochastic speckle pattern for the purpose of providing a surface that could be tracked for strain imaging purposes, as described in Section 2.2. A completed fill direction sample and warp direction sample are shown in Figure 5. The speckle pattern can be seen on the top surface of the warp direction sample. Sample dimensions, particularly widths and thicknesses, were then measured and recorded.

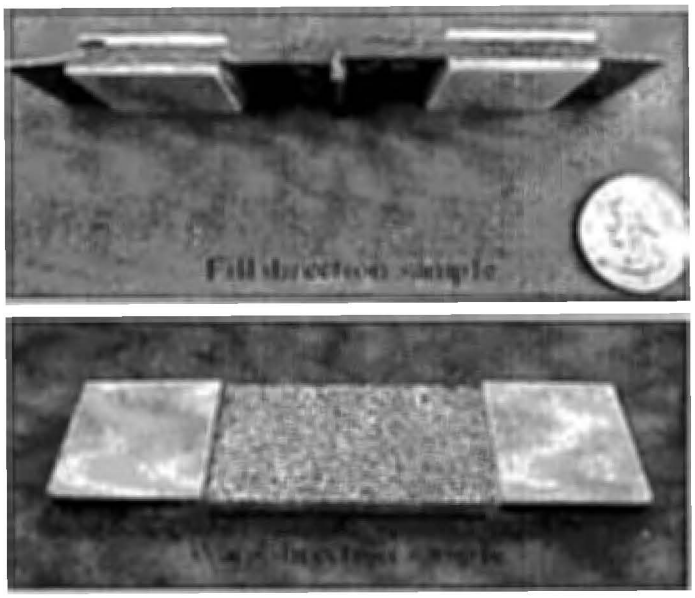

Figure 5: Completed fill and warp direction samples. In the upper image, the remaining fragment of the web section can be seen in the center of the sample.

2.2 Equipment

To determine the strain, digital image correlation (DIC) was performed using an Aramis™ strain visualization system. The DIC technique measures strain directly from the sample, completely independent of any compliance that may exist throughout the test system. DIC measures strain via tracking of identifiable features on the sample (or on the grips) throughout the image sequence. The stochastic pattern that was sprayed onto these samples provided the locally unique contrast and texture through which a superimposed grid of markers in the software was able to track the surface deformation. Since this is a full-field strain measurement, local strain and modulus information from anywhere on the deformed surface can be gleaned. This technique is particularly useful in this study since the thicknesses and fiber-derived constitutive properties vary greatly across the gauge sections. The Aramis™ system consists of two cameras, two light sources and a software-based geometric calibration which incorporates the precise relative angles and focal distances of the cameras to provide 3-dimensional displacement information. The prepared samples were tested using an Instron 4485 electromechanical universal testing system equipped with a 20,000 lb load cell. An image of the system is shown in Figure 6.

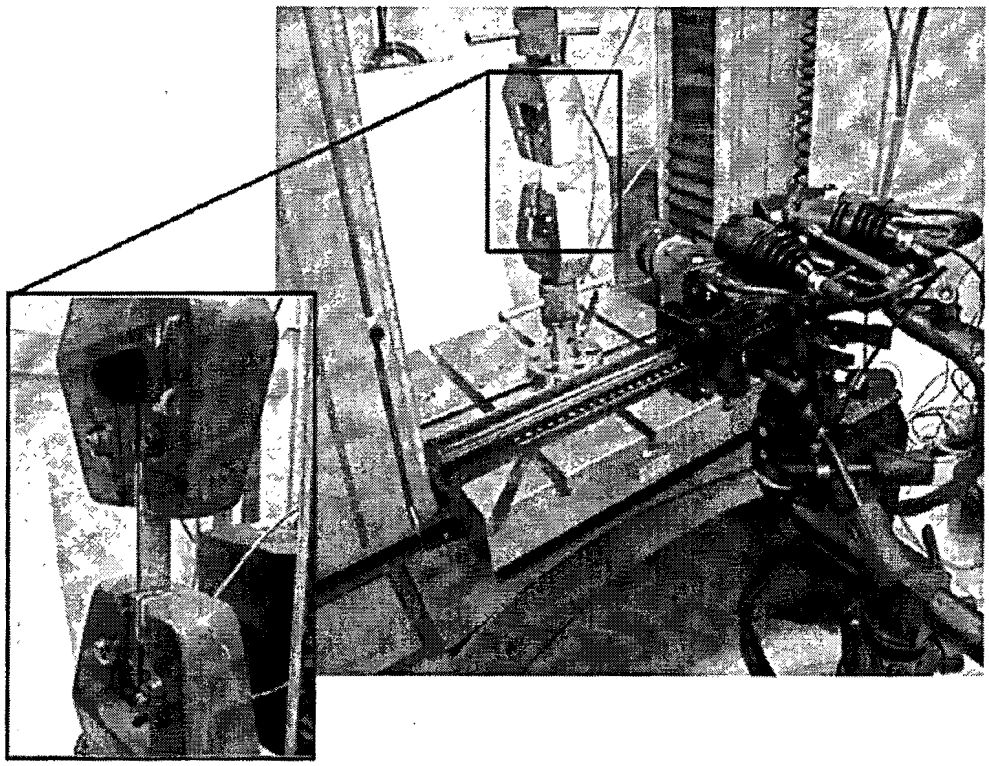

Figure 6: Mechanical test system showing sample loaded into the grips (inset) and the Aramis™ DIC system placed in front of the test region.

2.3 Test Procedure

During the test, the DIC system captured images at a rate of one frame per second. Load data was also collected simultaneously through the Instron load cell and was later correlated with the

strain data. The samples were loaded at a constant displacement rate of 0.05"/min (0.127 cm/min) until failure.

2.4 Analysis

To determine the elastic modulus for a given sample, the DIC local surface strain (specifically, the component of strain along the loading direction) was averaged across a selected region. For the warp direction coupons, the entire surface between the grips was averaged and reported as one value. Regions of poorly tracked cells along edges or near grip epoxy lines were excluded. An example of this strain selection for a warp direction sample is shown in Figure 7.

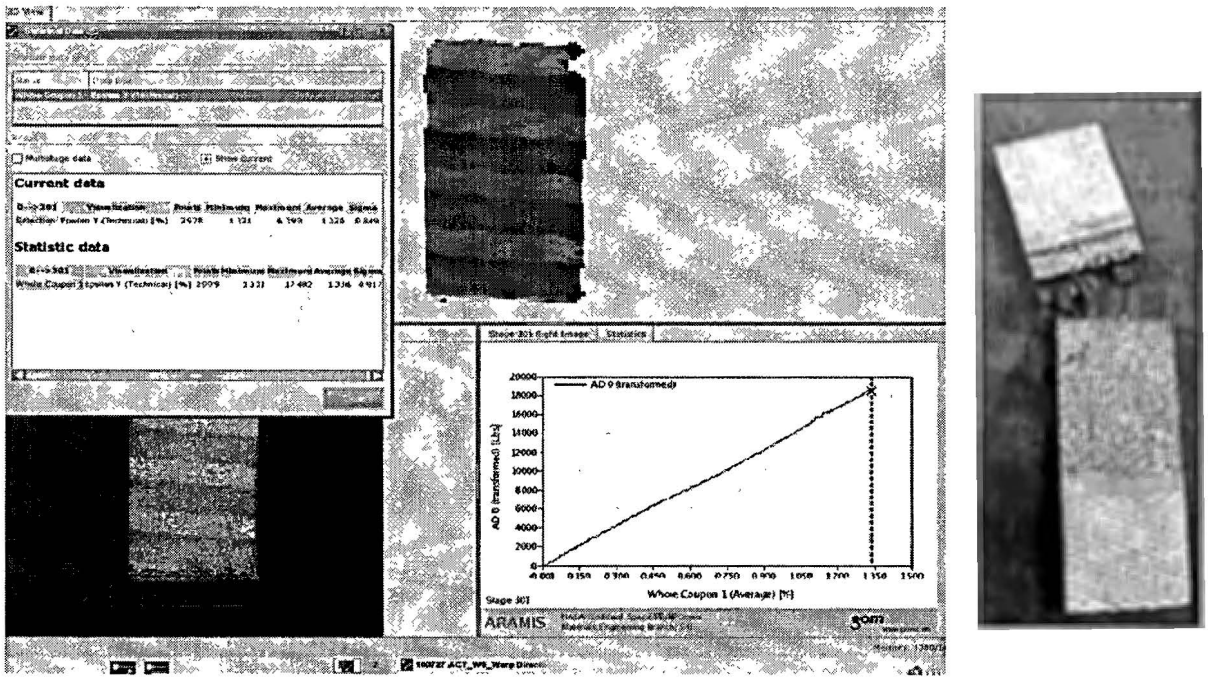

Figure 7: Screen capture of software showing the strain in the loading (warp) direction superimposed on the sample (lower left), the mean value statistic from the selected region (upper left and right), and statistical plot showing the load versus the mean strain. The image to the right shows the actual sample after failure.

For the fill direction coupons, the modulus was computed for the flats on both sides of the joint. The center of the coupon, i.e. the joint, was not included in either measurement as this region would have local properties distinct from the adjoining flats. The moduli for both flats were averaged to provide one modulus for each fill direction sample. An example of this strain selection for a fill direction sample is shown in Figure 8.

Figure 8: Screen capture of software showing the strain in the loading (fill) direction superimposed on the sample. For the fill direction samples, the mean value statistics from both sides of the joint were collected (note box outlining the upper flat). The image to the right shows the actual sample after failure.

3. RESULTS

3.1 Individual Test Results

For each individual test, one ultimate load value and one modulus value was reported. Figure 9 through Figure 12 show the results for the different weave configurations for both the warp and fill fiber directions.

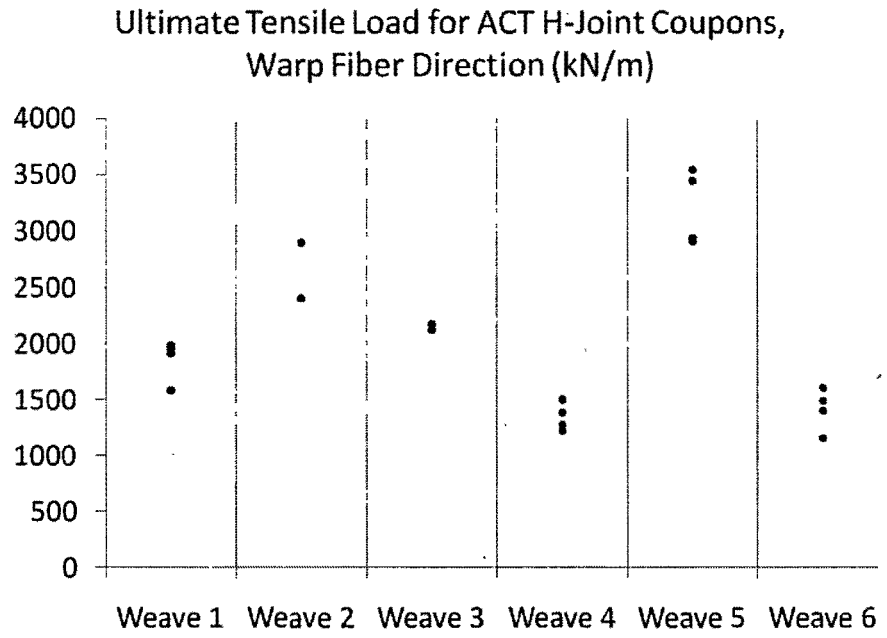

Figure 9: Average values of the ultimate tensile load reported from all samples tested from the warp fiber direction. At least 4 tests were completed for each weave configuration. For Weave 2, duplicate values are reported for each of the two observed data points. For Weave 3, only two data points are shown as the other two tests yielded corrupt data.

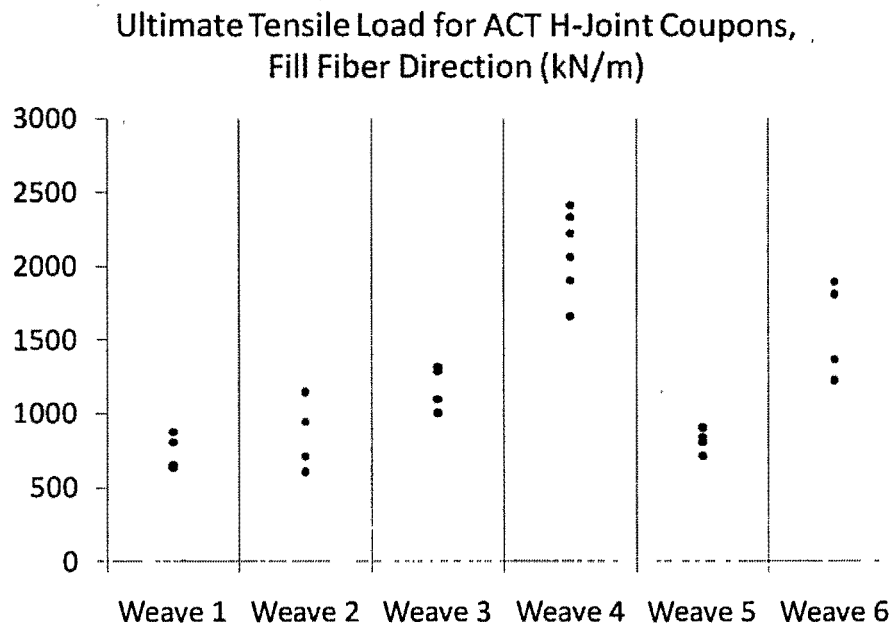

Figure 10: Average values of the ultimate tensile load reported from all samples tested from the fill fiber direction. At least 4 tests were completed for each weave configuration (Weave 4 contains 6 tests).

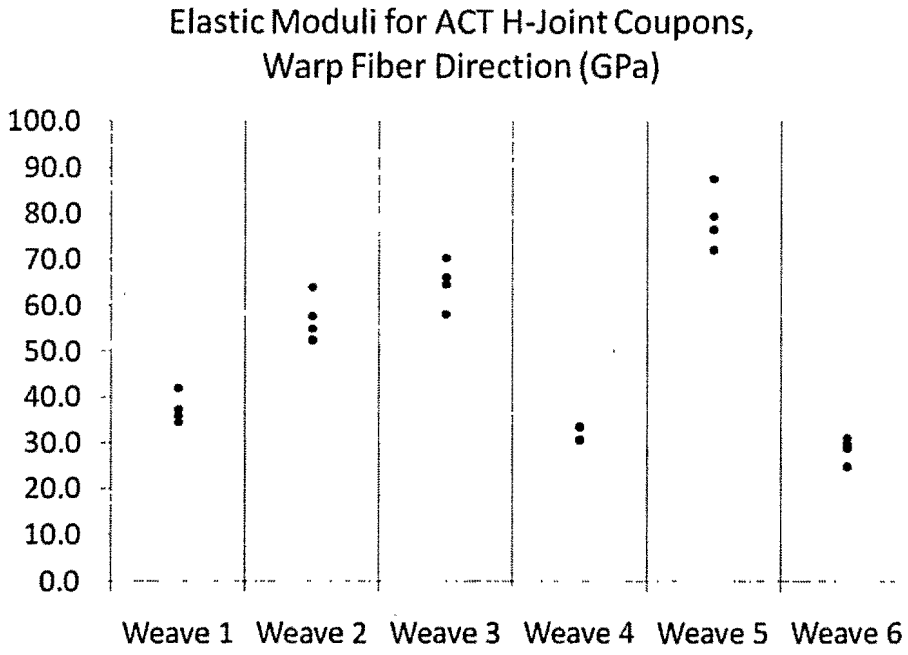

Figure 11: Average values of the elastic modulus reported from all samples tested from the warp fiber direction. At least 4 tests were completed for each weave configuration. For Weave 4, duplicate values are reported for each of the two observed data points.

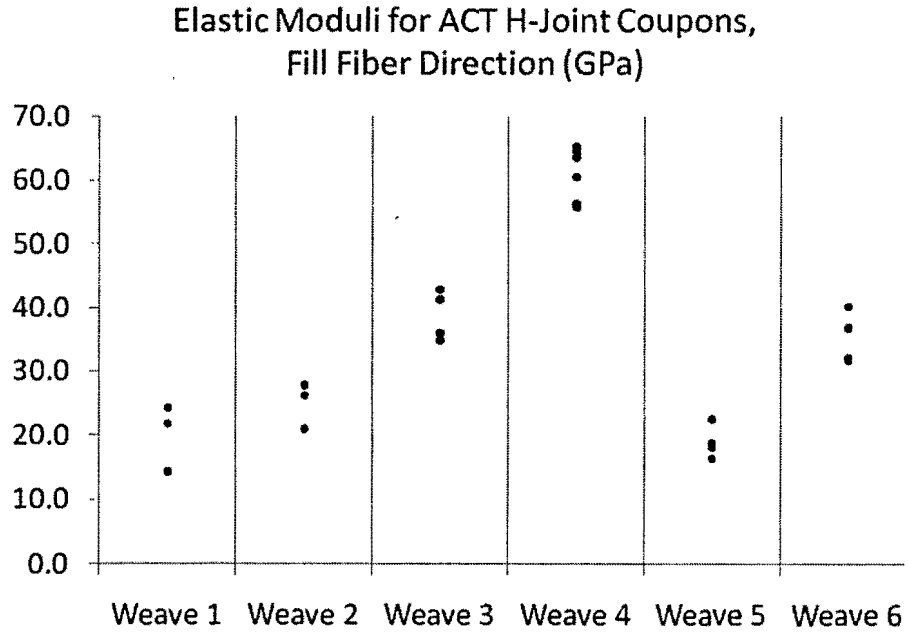

Figure 12: Average values of the elastic modulus reported from all samples tested from the fill fiber direction. At least 4 tests were completed for each weave configuration (Weave 4 contains 6 tests). For Weave 2, one data point was repeated in a subsequent test.

3.2 Weave Comparisons: Group Averages

The ultimate loads and moduli from all tests within a particular weave configuration were averaged into one value. These averages are reported here.

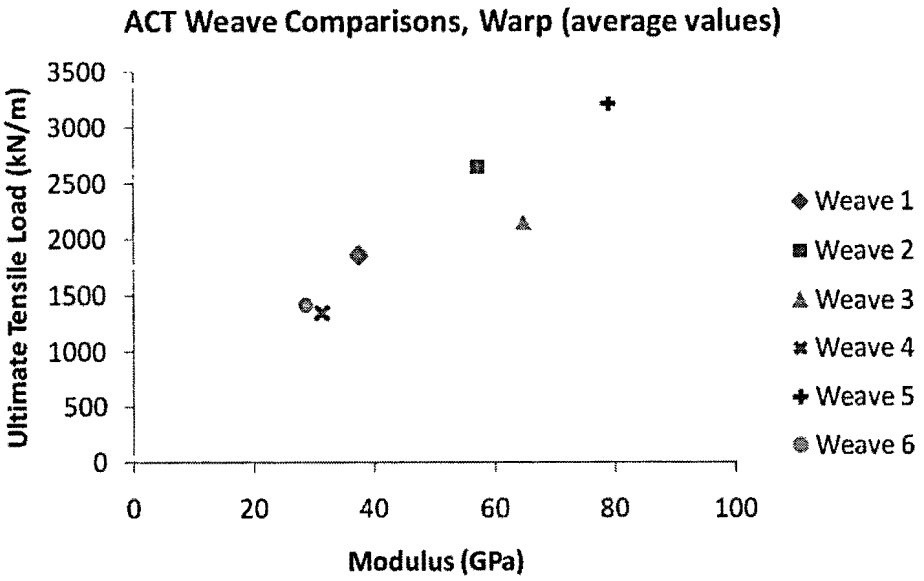

Figure 13: Group averages for all warp direction specimens from each weave, plotted as the ultimate tensile load versus the elastic modulus.

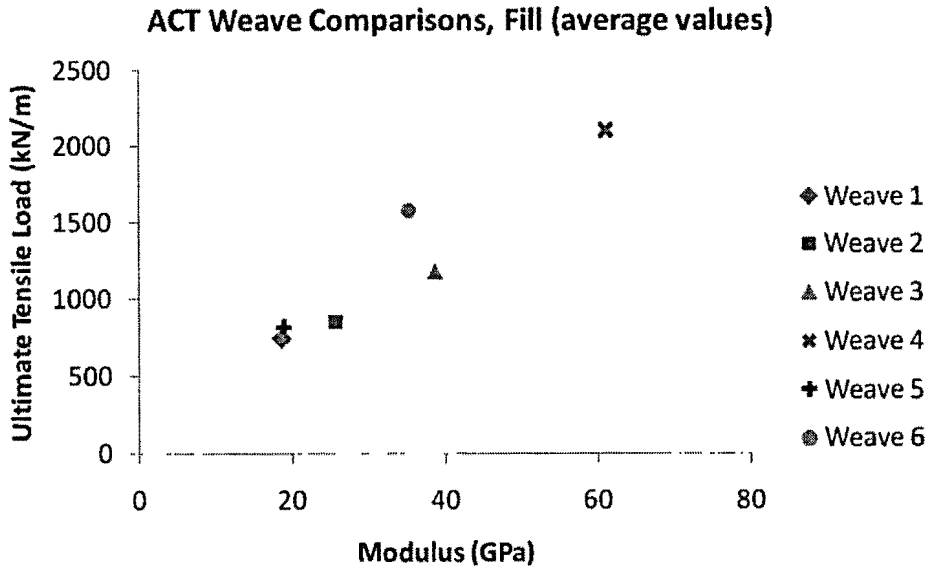

Figure 14: Group averages for all fill direction specimens from each weave, plotted as the ultimate tensile load versus the elastic modulus.

4. CONCLUSIONS

4.1 Weave Architecture Comparisons

As expected, the ratio of warp/fill fiber has a direct influence on strength and modulus. Weave 4 (25/75, z-fiber) demonstrates the highest strength and stiffness in the fill direction. Weave 5 (75/25, z-fiber) demonstrates the highest strength and stiffness in the warp direction. Weave 3 (50/50, z-fiber) falls in the middle. The weaves containing the z-fiber architecture performed better overall than the fully interlocked weaves with comparable fiber bias: Weave 4 out-performs Weave 6 (each has 25/75 bias) and Weave 3 out-performs Weave 1 (each has 50/50 bias). In addition, the hybrid weave performs better overall than the fully interlocked weave with comparable fiber bias (though the strength values in the fill direction are similar); Weave 2 out-performs Weave 1 (each has 50/50 bias). For axially loaded joint applications, the Weave 4 fiber configuration is the best overall candidate.